Cluster explosion in an intense laser pulse: Thomas-Fermi model

Marian Rusek,[1,2] Hervé Lagadec,[1] and Thomas Blenski[1]
[1]*Commissariat à l'Energie Atomique, DSM/DRECAM/SPAM, Centre d'Etudes de Saclay, 91191 Gif-sur-Yvette, France*
[2]*Instytut Fizyki, Polska Akademia Nauk, Aleja Lotników 32/46, 02-668 Warszawa, Poland*
(Received 26 May 2000; published 11 December 2000)

A refined three-dimensional version of the time-dependent Thomas-Fermi model is used to qualitatively study the explosion of rare-gas atomic clusters in an intense laser field. Clusters as large as 55 atoms are exposed to a strong subpicosecond laser pulse. A stepwise character of the explosion is observed in which atomic shells are expelled sequentially. The role of ''hot'' electron dynamics in the explosion process is also investigated via initial temperature effects. Contrary to previous opinions it seems that the so-called hydrodynamic explosion scenario is important for most energetic ions coming from the outermost shells only.

DOI: 10.1103/PhysRevA.63.013203 PACS number(s): 36.40.−c, 32.80.Rm, 42.50.Hz, 07.05.Tp

I. INTRODUCTION

Investigations of the interaction of atoms with short (duration $\tau \leqslant 1$ ps), intense (intensity $I > 10^{15}$ W/cm^2) laser pulses have led to the discovery of several interesting phenomena. Examples are excess photon or above-threshold ionization, suppression of ionization rate at high intensity (stabilization), generation of extreme ultraviolet and x radiation, and production of multiply charged atomic ions (for a review, see, e.g., [1]). In the case of such intensities the electric field of the laser radiation becomes comparable with the Coulomb field strength experienced by an electron in the ground state of atomic hydrogen. Thus a simple perturbative picture of the interaction of individual electrons with the field is no longer applicable.

One of the main motivations behind these studies was probably the desire to generate particles (photons, electrons, and ions) with energies much larger than the energy of a single laser photon. However, in gaseous media the absorption of laser energy is rather weak and the application of such media to the effective conversion of laser light into ultraviolet and x radiation is problematic. On the other hand, in solid media the absorption of laser energy is usually very good but the drawback of solid targets is that they are not as easily penetrated by the laser beam as gaseous media. Recently, atomic clusters formed in expanding high-pressure gas jets have been proposed as an alternative solution combining the advantages of both gaseous media (easily penetrated by a laser beam) and solid targets (large absorption of laser energy) [2]. The clusters may be considered as targets of intermediate size between gaseous media and solid targets.

Due to collective many-body effects the laser interaction with the atomic clusters (consisting of a few hundred to a few thousand atoms) may differ substantially from that of simple atomic and molecular systems. For instance, recent experiments on clusters irradiated by intense laser pulses have revealed several extremely high-energetic phenomena not encountered in previous experiments restricted to atoms and small molecules: efficient generation of highly charged atomic ions [3–9], generation of electrons and ions with MeV kinetic energies [7,8,10–12], and emission of intense x rays [3,5,13,14].

Several theoretical models have been proposed to explain the mechanism underlying the production of highly charged energetic ions in interaction of atomic clusters with intense laser pulses. In the phenomenological microplasma model [2,8] the cluster is treated as a spherical plasma and described by hydrodynamic equations. The Coulomb expansion of this plasma is effectively boosted by heating through collisions of the laser driven electrons with the ions (or inverse bremsstrahlung). In this model the charge states of the ions are governed mainly by collisional and tunnel ionization and impact with the very hot electrons. In Monte Carlo simulations of cluster explosion [15] an ionization ignition mechanism has been proposed. In this picture the enhanced rate of over-the-barrier ionization stems from the combined field of the laser and the Coulomb attraction from neighboring ions. When the intensity of the laser wave becomes sufficiently large, ions are rapidly stripped of electrons. Last but not least, in the coherent electron motion model [16], high charge states arise from impact ionization by coherently moving electrons.

Much work has been done also on the description of metal clusters within both quantal [17,18] and semiclassical [19,20] mean-field models based on the density-functional theory. In the case of metals with a simple electronic structure (e.g., sodium) only the valence electrons need to be treated explicitly and the nucleus together with the core electrons can be described by a pseudopotential that is effectively local. This approximation leads to a considerable simplification of the theoretical description of the electronic system. Recently, both ground state configurations and photoabsorption spectra of sodium clusters [18] as well as the dynamical evolution of electrons and ions in a sodium cluster irradiated by intense femtosecond laser [17] were investigated using such a theoretical approach based on density-functional theory within the local density approximation.

In this paper we develop a simple yet reasonably realistic theoretical approach to explosions of rare-gas atomic clusters in intense laser pulses. Our studies are based on a time-dependent Thomas-Fermi model, which may be considered as a semiclassical approximation (described by a Bloch-like hydrodynamic model) to the rigorous quantum dynamics of an electron gas. The results of previous papers [21,22] dealing with a one-dimensional version of a similar model are

now substantially extended and encompass the three-dimensional (3D) case explicitly. This allows us to describe the shell structure of real clusters in a natural way. Moreover, in one dimension a softening of the Coulomb potential $1/x$ is necessary to eliminate the unavoidable singularity at $x=0$. For sufficiently large clusters this soft Coulomb potential may alter the process of Coulomb explosion significantly. The 3D calculations presented in this paper avoid these difficulties and use the true Coulomb potential $1/r$. In addition, previous calculations [21,22] utilized a simplified version of the kinetic energy functional in the Thomas-Fermi model ρ^2 (ρ is the electron density). This approximation, although not very realistic, allows linearization of all equations of motion and easy solution using, e.g., a fast Fourier transform. In the present paper we use the correct nonlinear Thomas-Fermi kinetic energy functional $\rho^{5/3}$ valid for a 3D ideal electron gas at $T=0$. Some nonzero initial temperature effects are also investigated and discussed.

In principle the complete description of clusters in intense laser fields requires a solution of the time-dependent Schrödinger equation for many-electron systems. However, the solution of such an equation is beyond the capabilities of current computers. Even for two-electron systems in strong fields, *ab initio* wave-function studies require an extremely powerful computer and are only at the initial stage [23,24]. Nevertheless, the main qualitative features of several strong-field phenomena in multielectron atoms, like, e.g., high-order harmonic generation, can be obtained in simple models that invoke the picture of one active electron under the influence of an effective potential (see, e.g., [25–27]). On the other hand, however, the production of highly charged energetic ions by laser irradiation is of an essentially many-electron character and thus requires a theoretical framework within which a large number of electrons could be treated. The time-dependent Thomas-Fermi model used in this paper provides such a framework.

This paper is organized as follows. In Sec. II the Thomas-Fermi model of an atom is recalled and extended in order to describe stable rare-gas atomic clusters with van der Waals bonds. In Sec. III we assume that the oscillations of the electron cloud in a rare-gas atomic cluster can be viewed as a motion of a fluid characterized by density and velocity fields. This hydrodynamic formulation allows us to generalize the Thomas-Fermi model from Sec. II to the description of time-dependent phenomena in strong laser pulses. In Sec. IV the smooth particle hydrodynamics scheme is adapted to the description of the electron fluid in atomic clusters. Details of numerical implementation are presented. In Sec. V numerical experiments on cluster explosion are performed. A physical interpretation of the results obtained is also proposed. Finally, some comments and conclusions are given in Sec. VI.

II. THOMAS-FERMI MODEL

The earliest and the simplest of the density-functional methods [28,29] is the Thomas-Fermi model. It was introduced in the mid 1920s by Thomas [30] and independently by Fermi [31] in order to describe the self-consistent potential of multielectron atoms (for a review see, e.g., [32,33]). The advantage of this model is its simplicity (the atomic number Z is the only parameter) and universality (different atoms differ by scaling units only). In this model the ground state of a many-electron atom is described by the average electron density $\rho(\vec{r})$ and obtained by minimization of the electronic energy functional:

$$\mathcal{E}[\rho(\vec{r})]=\int d^3r\,\rho(\vec{r})U(\vec{r})-\frac{1}{2}\int d^3r\,e\,\rho(\vec{r})\phi(\vec{r}) - \int d^3r\frac{Ze^2\,\rho(\vec{r})}{|\vec{r}|}, \tag{1}$$

where the electrons interact through the self-consistent Coulomb potential

$$\phi(\vec{r})=-\int d^3r'\frac{e\,\rho(\vec{r}')}{|\vec{r}-\vec{r}'|}, \tag{2}$$

and the relations for the internal (kinetic) energy of an ideal electron gas at temperature T [34] are used locally (in the approximate expression below, T is assumed to be small),

$$U(\vec{r})=c_k[\rho(\vec{r})]^{2/3}+\frac{3\pi^2}{20}\frac{(kT)^2}{c_k[\rho(\vec{r})]^{2/3}}+\cdots, \tag{3}$$

where

$$c_k=\frac{3}{5}\frac{\hbar^2}{2m}[3\pi^2]^{2/3} \tag{4}$$

(e is the elementary charge and m denotes the electron mass).

The first term on the right hand side of Eq. (1) is the total internal energy of the electron gas, which is essentially of a quantum nature and as opposed to that of a classical gas does not vanish at $T=0$. The second term describes the Coulomb energy of the mutual interactions between the electrons through the self-consistent Coulomb potential, and the last term is the energy of the Coulomb interactions between the electrons and the nucleus.

The minimum of the energy functional in Eq. (1) can be obtained from the variation principle with the subsidiary condition

$$\int d^3r\rho(\vec{r})=Z \tag{5}$$

ensuring that the total number of electrons is constant. It is easy to verify that, up to the term of the order of T^2, the variation of the functional obtained after inserting the perturbative expansion from Eq. (3) into Eq. (1) yields the same result as variation of the nonzero temperature Thomas-Fermi free-energy functional (see, e.g., [35,36]).

As shown by Teller [37], the ground state of a system of interacting Thomas-Fermi atoms corresponds to the situation in which all the internuclear separations are infinite. It is known [38,33] that, in order to mimic a stable molecular binding within the Thomas-Fermi theory, it is necessary to

TABLE I. Total number of atoms in rare-gas atomic clusters consisting of different numbers of shells.

Number of shells	Number of atoms
1	13
2	55
3	147

add a so-called von Weizsäcker correction to Eq. (1). However, this correction is proportional to the gradient of density which makes it difficult to compute numerically (it is also of the order of terms dropped out in the smooth particle hydrodynamics method we use in Sec. IV). Moreover, what is even more important, the meaning of such a correction in time-dependent situations would be unclear. Therefore, in order to stabilize the cluster before the head of the pulse arrives we resort to a very simple approach and artificially diminish the Coulomb interaction between the nuclei (while the electron-electron and electron-nucleus interactions are not changed). This is done by lowering the charge of each nucleus as experienced by other nuclei by a small factor $\epsilon \ll 1$ (in this paper we use the value of $\epsilon = 10^{-2}$).

Thus, we assume that the ground state of a rare-gas atomic (van der Waals) cluster is described by the average electron density $\rho(\vec{r})$ and the equilibrium positions of the nuclei $\{\vec{R}_a\}$, which can be obtained by minimization of the following energy functional:

$$\mathcal{E}[\rho(\vec{r}),\{\vec{R}_a\}] = \int d^3r\, \rho(\vec{r}) U(\vec{r}) - \frac{1}{2}\int d^3r\, e\, \rho(\vec{r})\phi(\vec{r}) - \sum_{a=1}^{N} \int d^3r \frac{Ze^2\rho(\vec{r})}{|\vec{r}-\vec{R}_a|} + (1-\epsilon)\sum_{\substack{a,b=1 \\ a>b}}^{N} \frac{(Ze)^2}{|\vec{R}_a-\vec{R}_b|}. \quad (6)$$

It differs from the single-atom functional (1) by adding summation over different nuclei and an additional term that represents the energy of the electrostatic interactions between the nuclei modified by a factor $(1-\epsilon)$.

Ground state properties of small clusters of rare-gas atoms have been investigated extensively in the literature (see, e.g., [39–41]). The usual theoretical approach is to describe the atoms in a cluster as a system of particles interacting via a short-range potential such as the Lennard-Jones potential. It has been reported that particularly stable configurations of such clusters are of the form of closed-shell icosahedra. In this case the number of atoms per shell N_s is related to the shell number s by the relation $N_s = 10s^2 + 2$. Table I shows the total number of atoms $N = \Sigma_s N_s + 1$ in clusters consisting of different numbers of shells (note that there is an additional atom in the middle of the icosahedron).

As a simple example let us briefly consider the case of $U = (A/2)\rho$ (this approximation was used in [21,22]). It is readily seen that in the case of neutral atoms the electrostatic potential is related to the electron density by $\Phi = (A/e)\rho$. Solving the Poisson equation, we get the following expression for the ground state density:

$$\rho = \frac{Z\,e^2}{A}\sum_{a=1}^{N} \frac{e^{-\kappa|\vec{r}-\vec{R}_a|}}{|\vec{r}-\vec{R}_a|}$$

where $\kappa = \sqrt{4\pi e^2/A}$. Thus within the Born-Oppenheimer approximation two neutral atoms separated by a distance R interact with each other via a Yukawa-type potential modified by the charge defect, $\Phi'(R) = Ze(e^{-\kappa R} - \epsilon)/R$. Our numerical experiments indicate that in this case also the icosahedral structure seems to provide the minimal energy.

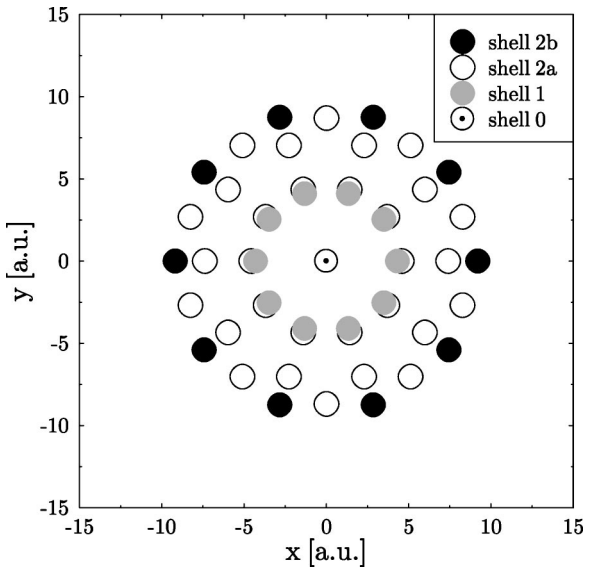

FIG. 1. Initial guess for the equilibrium positions of the nuclei $\{\vec{R}_a\}$ in an $N = 55$ atom rare-gas cluster. This structure consists of two closed icosahedral shells and an atom in the middle. Atoms belonging to different shells are marked by filled circles shaded in different ways. Shell 0 is the central atom. The second shell has been split into two subshells with different radii.

We prepared an initial state of the form of a two-shell icosahedron containing $N = 55$ atoms. The distance between neighboring atoms on each shell has been chosen to equal the equilibrium distance for two atoms given by the minimum of the potential Φ'. For the value $\epsilon = 10^{-2}$ used we get the equilibrium distance $R_0 \simeq 7\kappa^{-1}$ (note that it does not depend on Z). After solving the Newton equations of motion for point particles interacting via the potential Φ' with small friction terms added in order to have energy dissipation, we found a stable structure of the nuclei that also preserved the initial icosahedral symmetry (its energy was lower than the energy of the equilibrium structure coming from a random initial arrangement of atoms). However, the final distance between neighboring atoms turned out to be different for shells 1 and 2 (it is slightly lower for the inner shell). The results are shown in Fig. 1. They will be used as input into the hydrodynamic calculations involving the motion of an electron fluid presented in Sec. V. To choose the length scale on this figure we assumed that $\kappa^{-1} = 1$ a.u. In this case the

equilibrium distance between two atoms is $R_0 \simeq 7$ a.u. $= 3.7$ Å, which is similar to the spacing of atoms in argon clusters [42].

III. HYDRODYNAMIC FORMULATION

The time-dependent density functional theory is a nontrivial extension of the steady-state density functional theory to the time domain [43–48]. Usually this theory is used in the regime of weak fields for which perturbation theory is applicable. Nevertheless, recently several applications of this theory to the nonperturbative treatment of atoms, molecules, and solids in intense laser fields have appeared [49]. One example is the study of harmonic generation in He atoms [50]. However, the numerical solution of the time-dependent Kohn-Sham equations is very time consuming even in the case of helium atoms. Thus for a description of cluster explosion an alternative approach should be sought. Following Bloch [51] we assume that the oscillations of the electron cloud in a rare-gas atomic cluster can be viewed as a motion of a fluid characterized by density $\rho(\vec{r},t)$, velocity field $\vec{v}(\vec{r},t)$, and internal energy $U(\vec{r},t)$, obeying the standard conservation equations for number of particles, momentum, and energy. In the Lagrangian form, they are written

$$\frac{d\rho(\vec{r},t)}{dt} = -\rho(\vec{r},t)\vec{\nabla}\cdot\vec{v}(\vec{r},t), \tag{7a}$$

$$m\frac{d\vec{v}(\vec{r},t)}{dt} = -\frac{1}{\rho(\vec{r},t)}\vec{\nabla}p(\vec{r},t) + e\vec{\nabla}\Phi(\vec{r},t), \tag{7b}$$

$$\frac{dU(\vec{r},t)}{dt} = -\frac{p(\vec{r},t)}{\rho(\vec{r},t)}\vec{\nabla}\cdot\vec{v}(\vec{r},t), \tag{7c}$$

where the pressure p is defined by the equation of state for an ideal fermion gas [34],

$$p(\vec{r},t) = \frac{2}{3}\rho(\vec{r},t)U(\vec{r},t), \tag{8}$$

and the self-consistent Coulomb potential reads as

$$\Phi(\vec{r},t) = \phi(\vec{r},t) + \sum_{a=1}^{N}\frac{Ze}{|\vec{r}-\vec{R}_a(t)|}. \tag{9}$$

A similar hydrodynamic model has been used in the weak-field limit for the study of photoabsorption of an atom in free space [52] and in plasma [53], and more recently (in its one-dimensional version) for the study of atoms, molecules, and small clusters exposed to an intense laser pulse [21,22].

The hydrodynamic equations (7) for the electron density ρ should be supplemented by the Newton equations of motion for the positions of the nuclei $\vec{R}_a$:

$$M\frac{d^2\vec{R}_a(t)}{dt^2} = -Ze\vec{\nabla}\Phi'(\vec{R}_a(t),t), \tag{10}$$

where

$$\Phi'(\vec{R}_a(t),t) = \phi(\vec{R}_a(t),t) + (1-\epsilon)\sum_{\substack{b=1\\ b\neq a}}^{N}\frac{Ze}{|\vec{R}_a(t)-\vec{R}_b(t)|} \tag{11}$$

is the modified Coulomb potential and M denotes the nuclear mass.

The interaction with the laser pulse is treated within the dipole approximation by replacing the electrostatic Coulomb potential in Eqs. (7) and (11) by

$$\phi(\vec{r},t) \to \phi(\vec{r},t) - \vec{r}\cdot\vec{\mathcal{F}}(t), \tag{12}$$

where $\vec{\mathcal{F}}(t)$ is the electric field of the incoming wave. The linearly polarized wave of the pulse used in the simulations is assumed to have a field envelope proportional to sine squared with a full width at half maximum τ and an optical period τ_0:

$$\vec{\mathcal{F}}(t) = \vec{\mathcal{F}}_0 \sin^2\left(\frac{\pi}{2\tau}t\right)\cos\left(\frac{2\pi}{\tau_0}t\right). \tag{13}$$

The initial values of the electron density $\rho(\vec{r},t_0)$ and the equilibrium positions of the nuclei $\{\vec{R}_a(t_0)\}$ are obtained by minimization of the Thomas-Fermi energy functional (6) from Sec. II. The electron fluid is initially considered as a static one, i.e., $\vec{v}(\vec{r},t_0)\equiv\vec{0}$. Finally, the values of $U(\vec{r},t_0)$ are calculated using the relation Eq. (3) for the internal energy of a uniform electron gas at a given temperature $T=T_0$. This relation, which is used at the initial time $t=t_0$ only, can be considered as the sole ''quantum-mechanical'' ingredient in the present model [Eq. (8) holds for both a classical and quantum gas].

In practice, the ground state structure of a cluster corresponding to the minimum of the Thomas-Fermi energy functional Eq. (6) can be obtained in a convenient way by looking for the stationary solution of the hydrodynamic equations (7) with small viscosity terms added, supplemented by the Newton equations (10) with small friction terms added. Let us mention that in order to obtain in this way the equilibrium state structure of a cluster corresponding to the nonzero temperature of the electron gas $T>0$ it is necessary to directly substitute Eq. (3) into Eq. (8) and solve only the first and second of Eqs. (7). Indeed, it follows from the first and third of Eqs. (7) that

$$\frac{U(\vec{r},t)}{[\rho(\vec{r},t)]^{2/3}} = \frac{U(\vec{r},t_0)}{[\rho(\vec{r},t_0)]^{2/3}}. \tag{14}$$

According to Eq. (3) this means that a system prepared initially at $T_0=0$ will remain at this constant temperature $T=T_0$ all the time. This is, however, not the case if $T_0>0$.

IV. SMOOTH PARTICLE HYDRODYNAMICS

The time-dependent Thomas-Fermi model presented in the previous section involves fluids moving freely in 3D un-

der the influence of Coulomb and pressure forces. Usually these kinds of problems are best approached numerically using a Lagrangian formulation where the fluid is represented by a large number of particles. In this paper we use the probably most popular numerical scheme of this kind, known as smooth particle hydrodynamics (SPH) [54,55]. This simple and robust method to solve the hydrodynamic equations presents some clear advantages over more traditional grid-based Eulerian methods for calculations of fluid flows. Within SPH a completely gridless approach is used to compute the spatial derivatives. Thus it is easy to handle three-dimensional problems and problems without any particular symmetries. Moreover, calculations are performed in the relevant regions of space only. No computational time is spent in empty regions making SPH a very computationally efficient scheme.

The name of the method comes from the fact that the density at any point of space is obtained by summing up the contributions from n smoothed pseudoparticles,

$$\rho(\vec{r}) = \frac{ZN}{n} \sum_{j=1}^{n} f(\vec{r}-\vec{r}_j). \tag{15}$$

The function f is assumed to be spherically symmetric $f(\vec{r}) = f(|\vec{r}|)$ and normalized $\int d^3r f(\vec{r}) = 1$. The SPH is a particle-based approach to hydrodynamics. The computational elements are not grid cells, as in finite difference methods, but moving points in space where computational data in the fluid are sampled. The transition between field quantities $F(\vec{r})(F=\rho,\vec{v},U,\Phi,\ldots)$ and pseudo-particle-based quantities F_i can be done in the following way:

$$F_i = \int d^3r\, f(\vec{r}-\vec{r}_i)\, F(\vec{r}). \tag{16}$$

The SPH method is accurate up to second order in the characteristic width d of the kernel function f. Within this approximation the following useful rule of thumb holds: $(F\,G)_i = F_i\, G_i$.

The motion of the pseudoparticles and particle-based quantities is governed by the equations of the fluid. After inserting Eq. (15) using Eq. (16) and neglecting terms of the order of $O(d^2)$ one arrives at the discretized SPH version of the hydrodynamic Eqs. (7) (see, e.g., [56,57]):

$$\frac{d\vec{r}_i}{dt} = \vec{v}_i, \tag{17a}$$

$$m\frac{d\vec{v}_i}{dt} = -\sum_{j=1}^{n} \left(\frac{p_i}{\rho_i^2} + \frac{p_j}{\rho_j^2} \right) \vec{\nabla}_i w(\vec{r}_i-\vec{r}_j) + e\vec{\nabla}_i \Phi_i, \tag{17b}$$

$$\frac{du_i}{dt} = \frac{p_i}{\rho_i^2} \sum_{j=1}^{n} (\vec{v}_i-\vec{v}_j)\cdot\vec{\nabla}_i w(\vec{r}_i-\vec{r}_j), \tag{17c}$$

where

$$w(\vec{r}) = \frac{ZN}{n} \int d^3r'\, f(\vec{r}'-\vec{r}) f(\vec{r}'). \tag{18}$$

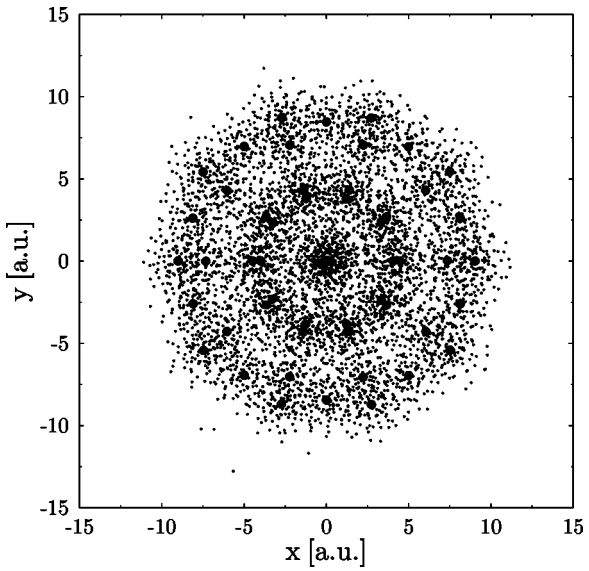

FIG. 2. Ground state structure of an $N=55$ atom cluster with $Z=1$. Equilibrium positions of the nuclei $\{\vec{R}_a\}$ are marked by filled circles. Small black dots correspond to the positions of the pseudoparticles modeling the equilibrium electronic density ρ.

Equations (17) should be supplemented by the SPH version of the equation of state (8):

$$p_i = \frac{2}{3}\rho_i\, u_i\,. \tag{19}$$

Thus the problem of solving the hydrodynamic equations (7) has been transformed into an n-body problem for the pseudoparticles. It is interesting to observe that in the simplified case of $u_i \propto \rho_i$ and $p_i = \rho_i\, u_i$ Eqs. (17) become the Hamilton equations of motion for the smoothed pseudoparticles Eq. (15) with the Hamiltonian given by the Thomas-Fermi energy functional (1).

The total Coulomb force experienced by pseudoparticle i can be written as a sum of all the individual forces:

$$\vec{\nabla}\Phi_i = \sum_{j=1}^{n} \frac{q(|\vec{r}_i-\vec{r}_j|)}{|\vec{r}_i-\vec{r}_j|^2} \frac{\vec{r}_i-\vec{r}_j}{|\vec{r}_i-\vec{r}_j|} - \sum_{a=1}^{N} \frac{Q(|\vec{r}_i-\vec{R}_a|)}{|\vec{r}_i-\vec{R}_a|^2} \frac{\vec{r}_i-\vec{R}_a}{|\vec{r}_i-\vec{R}_a|} + \vec{\mathcal{F}}(t) \tag{20}$$

where

$$q(|\vec{r}|) = e\,4\pi \int_0^{|\vec{r}|} u^2 du\, w(u),$$

$$Q(|\vec{R}|) = Ze\,4\pi \int_0^{|\vec{R}|} u^2 du\, f(u). \tag{21}$$

The pressure forces in Eqs. (17) are short-range forces and only neighboring particles contribute to the local pressure gradients. This is not the case, however, with the long-range Coulomb force (20).

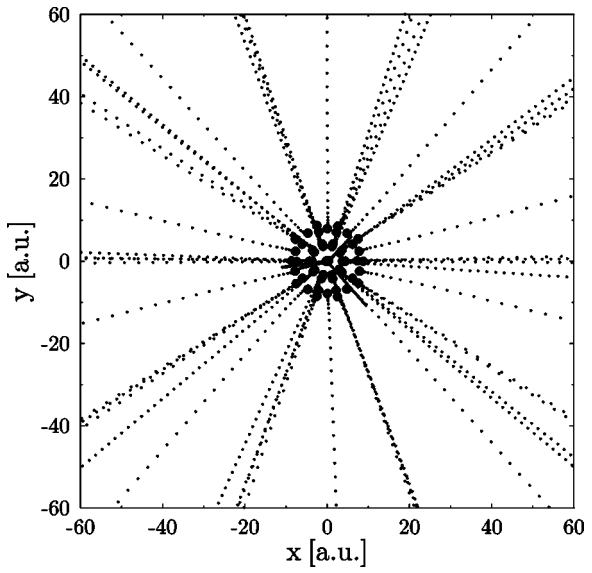

FIG. 3. Trajectories of the ions after explosion of the $N=55$ atom cluster from Fig. 2 exposed to a laser pulse. Small black dots correspond to the positions of the nuclei at every optical period. Initial positions of the atoms are marked by filled circles.

Using the simplest particle-particle method the forces between all pairs of pseudoparticles need to be calculated in order to evaluate the second term in expression (20). The time required to calculate all interactions is $O(n^2)$ and this is inefficient for systems with a large number of pseudoparticles n. Thus, in order to calculate the Coulomb force coming from the pseudoparticles we use a version of the tree-based method [58–61] instead. Within this method space is divided into cells organized in a form of a tree. When a particle is far enough from a cell the Coulomb force is calculated using the multipole expansion. For n pseudoparticles, only $O(n \log n)$ time is required (under certain assumptions). Tree-based methods can easily be merged with the smooth particle hydrodynamics scheme [62,63]. However, we still resort to the simple particle-particle method to calculate the Coulomb force coming from the nuclei [the second term in expression (20)].

In this paper we utilize f in the form of a Gaussian function:

$$f(\vec{r})=\left(\frac{\alpha}{\sqrt{\pi}}\right)^3 e^{-(\alpha\vec{r})^2}. \tag{22}$$

The parameter α from Eq. (22) is chosen to minimize the energy Eq. (1) of a Thomas-Fermi atom of given Z. It should also be regarded as a function of the number of pseudoparticles per atom n/N. For example, for $n/N=125$ (this is the value used later in the paper) we found a minimum of energy at $\alpha=3$ for $Z=1$ and $\alpha=7$ for $Z=18$. The ground state for each value of α was obtained by solving Eqs. (17) numerically with small friction terms added. Then the energy of all atoms was plotted as a function of α and a minimum picked up. Interestingly, at the value of α corresponding to this minimum of energy the Thomas-Fermi energy relations are preserved, i.e., $2\,\mathcal{E}_{\rm int}+\mathcal{E}_{\rm pot}=0$ [32] where $\mathcal{E}_{\rm int}=(ZN/n)\Sigma_j u_j$ is the internal energy of the electron gas [first term in Eq. (1)] and $\mathcal{E}_{\rm pot}=(ZN/n)\Sigma_j e\Phi_j$ is the potential energy of the electron gas [second and third terms in Eq. (1)].

V. CLUSTER EXPLOSION

Let us start the presentation of the results of our numerical simulations of cluster explosion within the time-dependent Thomas-Fermi model with a discussion of the case of $Z=1$. It is known, that within the static (time-independent) Thomas-Fermi model atoms of different atomic number Z differ by scaling units only. In the case of the time-dependent Thomas-Fermi model (including ion dynamics) the situation is much more complicated and to our knowledge there does not exist any simple scaling of the final energies and charges of ions with atomic number Z. Let us mention only that the Coulomb force acting on pseudoparticles in Eqs. (17) scales as Z whereas the pressure force scales as $Z^{2/3}$ (at

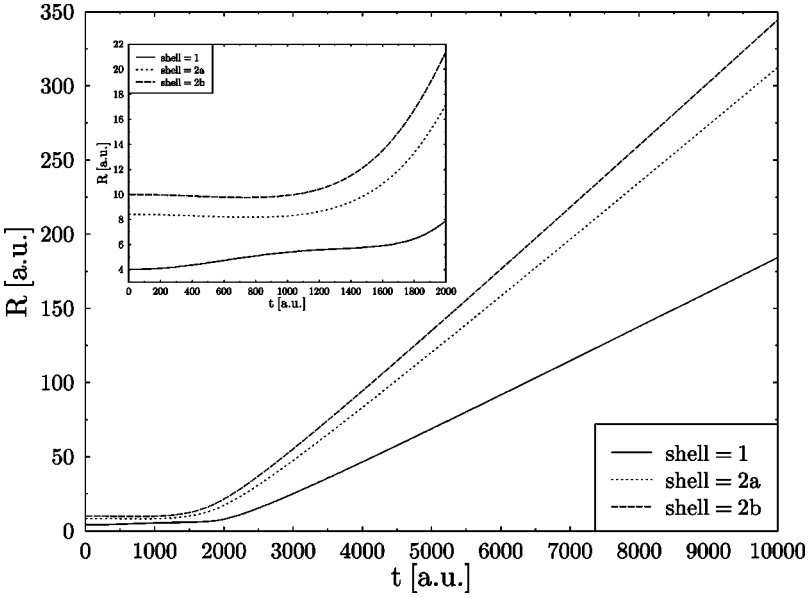

FIG. 4. Radii $\mathcal{R}$ of each (sub)shell of the cluster from Fig. 3 ploted versus time t. Inset corresponding to the magnification of a part of the original plot shows the details of the beginning stages of the explosion.

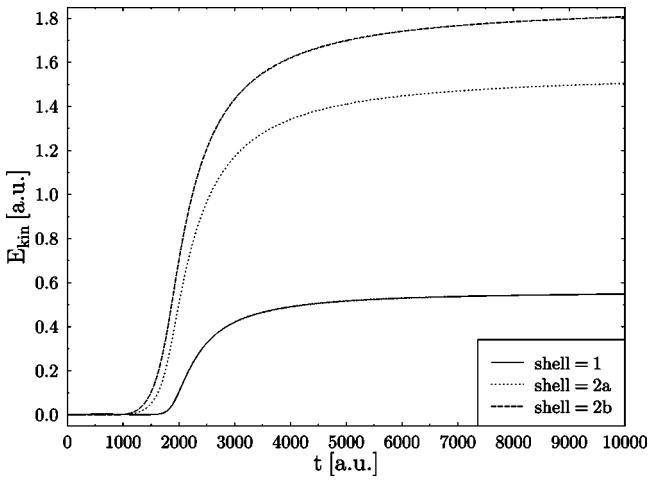

FIG. 5. Average kinetic energy $\mathcal{E}_{\rm kin}$ of the ions coming from different (sub)shells of the cluster from Fig. 3 ploted versus time t.

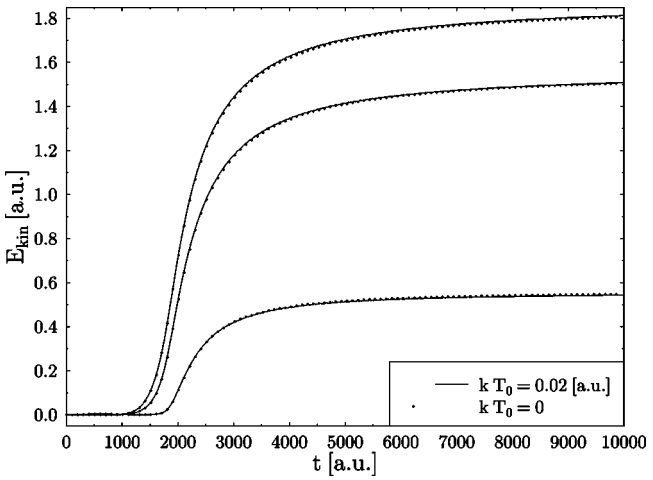

FIG. 6. Average kinetic energy $\mathcal{E}_{\rm kin}$ of the ions coming from different (sub)shells of an $N=55$ atom cluster versus time t plotted for different initial temperatures T_0 of the electron gas.

$T=0$). Nevertheless, we may expect that simulations performed for $Z=1$ will allow us to gain some basic qualitative information about the process of cluster explosion without spending too much computational time. Later on we plan also to consider briefly a more realistic case of $Z=18$ (argon clusters). This will allow us to compare the results coming from our model with the results of recent Monte Carlo simulations.

It turns out that the main problem in considering the case of $Z \gg 1$ comes not from the increase of Z but rather from the necessity to simultaneously increase the parameter α in Eq. (22) in order to fulfill the Thomas-Fermi energy relations (see the discussion at the end of Sec. IV). For instance, in the case of an argon cluster with atomic number $Z=18$ ($\alpha=7$) the maximal force acting on the pseudoparticles is about 200 times larger than in the case of $Z=1(\alpha=3)$. This makes the code about 20 times slower. In our code we use the fifth order Cash-Karp Runge-Kutta method with adaptive stepsize control (see, e.g., [64]) to integrate Eqs. (17) and (10) in time.

First we will need a ground state structure of an $N=55$ atom cluster with $Z=1$ at $T=0$ corresponding to the minimum of the energy functional given by Eq. (6) together with Eq. (3). It was obtained by solving simultaneously the SPH hydrodynamic equations (17) and the Newton equations (10) with small friction terms added. At the initial time we used the approximate values of the equilibrium positions of the nuclei $\{\vec{R}_a^{(0)}\}$ from Fig. 1. The initial guess for the electronic density was chosen in the form

$$\rho^{(0)}(\vec{r}) = \frac{Z e^2}{A} \sum_{a=1}^{N} \frac{e^{-\kappa|\vec{r}-\vec{R}_a^{(0)}|}}{|\vec{r}-\vec{R}_a^{(0)}|},$$

which corresponds to the simplified case of $p \propto \rho^2$ within the Born-Oppenheimer approximation (see the discussion in Sec. II). Pseudoparticles were initially distributed randomly with the density $\rho^{(0)}$. The resulting stationary positions of the pseudoparticles $\{\vec{r}_i\}$ describing the equilibrium electronic density ρ and the equilibrium positions of the nuclei $\{\vec{R}_a\}$ are depicted in Fig. 2. Note that the radii of all the shells of the cluster in Fig. 2 are slightly smaller than in Fig. 1. It is the inner shell that collapsed most with respect to the approximate structure of Fig. 1.

In the next step the cluster from Fig. 2 was exposed to a strong laser pulse with the peak intensity $I=1.4 \times 10^{15}$ W/cm^2 (or $\mathcal{F}_0=0.2$ a.u.). The pulse used in the simulations had a wavelength $\lambda=800$ nm (or $\tau_0=110.425$ a.u.) and a temporal full width at half maximum $\tau=106.67$ fs (or $\tau/\tau_0=40$). All of the results presented in this paper were obtained using a wave polarized linearly along the x axis. The only independent parameter left is the mass of the nuclei M, which has been set to $M/m=2000$. In Fig. 3 we present the trajectories of the ions after explosion of the cluster. The black dots correspond to the positions of the nuclei at every optical period. Larger filled circles represent the initial positions of the nuclei. We see that there is a forward-backward symmetry. The x axis (parallel to the polarization of the pulse) seems also to be a symmetry axis. In addition in Fig. 4 we plot the radii $\mathcal{R}$ of the shells of the cluster from Fig. 3 as a function of time t. These radii were computed as the average distance between each ion from a given shell and the central ion of the cluster. For convenience the second shell was split into two subshells with different initial radii (i.e., a subshell is defined as a group of atoms equally spaced from the central atom of the cluster). It is seen that the explosion is neither instantaneous nor uniform. It exhibits a layerlike structure in which shells of cluster ions are expelled sequentially. The inset corresponding to the magnification of a part of the original plot shows the details of the beginning stages of the explosion at $0 \leqslant t \leqslant 2000$ a.u.. It is interesting to see that it is the inner shell of the cluster that started to expand first and ''pushed'' the outer shells. In Fig. 5 we have the kinetic energy $\mathcal{E}_{\rm kin}$ of the atomic ion fragments versus time t. Again it is averaged over the different (sub)shells. Note once more the stepwise character of the explosion, the ions leaving first being far more energetic than those leaving later. Such a process has been suggested as an explanation of phenomena observed in ex-

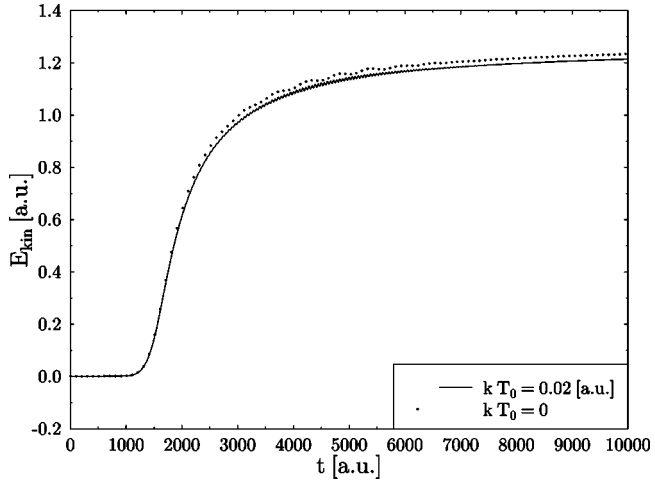

FIG. 7. Same as in Fig. 6 but for an $N=6$ atom cluster.

periments [9] and confirmed within 1D numerical simulations using a similar time-dependent Thomas-Fermi hydrodynamic model [21].

''Hot'' electron dynamics is believed to play an important role at the initial stages of the cluster explosion (see, e.g., [2,8]). In this picture electrons moving under the influence of a laser pulse expand and ''pull'' the cold heavy ions outward with them. This hydrodynamic pressure associated with the hot electrons together with Coulomb interaction are the two forces that act on the cluster, causing it to expand during and after the laser pulse. The hydrodynamic part of the cluster expansion results from a conversion of electron thermal energy into the directed kinetic energy of the ions. This expansion process can be perfectly described within the time-dependent Thomas-Fermi model used. However, instead of introducing some phenomenological coefficient describing the absorption of laser energy into the hydrodynamic equations (17) for an ideal electron fluid, in our paper we have chosen to investigate the effect of preheating the cluster *before* the pulse arrives. This is done in a natural way by introducing a small nonzero electron temperature T into Eq. (3) used at time $t=0$ in order to calculate the initial values $U(\vec{r},0)$ of the internal energy of the electron gas. We use an initial temperature of $k\,T_0=0.02$ a.u. (or $k\,T_0=0.3$ eV). In this case the initial values of u_i are changed by about 1% in the low-electron-density regions between the atoms and remain essentially unchanged in the high-density regions close to the atomic core [thus the perturbative expression (3) is perfectly justified]. In Fig. 6 we compare the kinetic energy $\mathcal{E}_{\rm kin}$ of the atomic ion fragments coming from the explosion of clusters prepared initially in equilibrium states at temperatures $T=T_0$ and $T=0$. It follows from inspection of this plot that ions coming from the outer shells of the cluster are indeed somewhat accelerated by thermal expansion of the electron gas. However, for ions originating from the inner shell the opposite is true: their energy turns to be lower when the initial temperature of the electron gas in the cluster is higher. To understand this effect we repeated the same calculations for an $N=6$ atom cluster with an initial octahedral structure consisting of one shell. The corresponding plot is presented in Fig. 7. We see that again the kinetic energy of the outgoing ions is lower for a higher initial temperature of the cluster. A possible explanation of this effect is that the space-charge ionization due to electrons has an important effect on the ion energies resulting from the cluster explosion. As electrons are liberated in small clusters they exit the volume of the cluster quite rapidly and thus cannot continue to ionize the atoms. It is reasonable to expect that this escape of electrons is accelerated by a nonzero initial temperature of the cluster; this results in a lower charge of the atoms, and thus the Coulomb explosion of small clusters and inner shells of larger ones is slowed down. A mixed Coulomb-hydrodynamic expansion behavior has been observed recently in the explosion of xenon clusters [9]. However, according to these authors most energetic ions arise from the

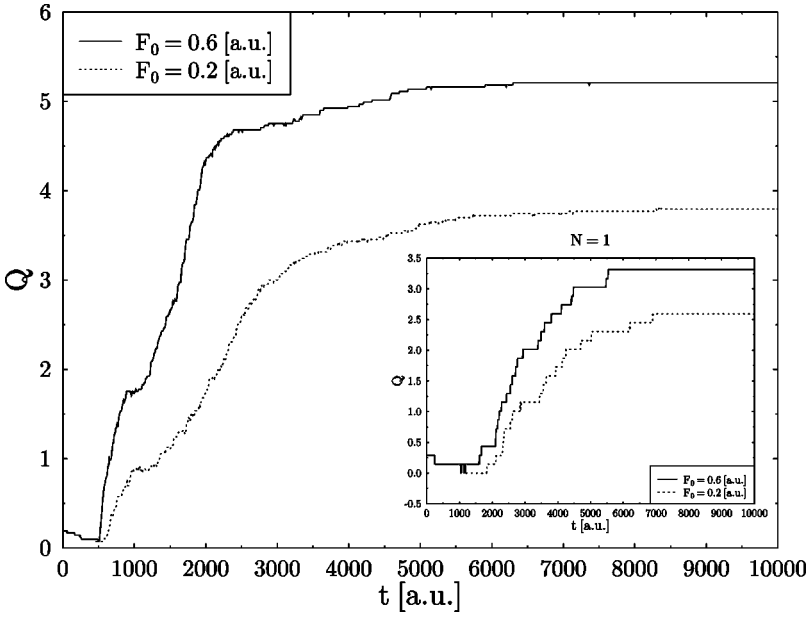

FIG. 8. Average charge $\mathcal{Q}$ of the ions after explosion of an $N=6$ atom cluster with $Z=18$ plotted versus time t for two different amplitudes $\mathcal{F}_0$ of the incoming laser pulse. Inset presents time dependence of the charge state of a single atom illuminated by the same laser pulse.

Coulomb and not the hydrodynamic scenario of the explosion. This seems to be the opposite of our results.

Finally, let us consider a more realistic case of $Z=18$ and $M/(Zm)=4045.45$ (argon clusters). Figure 8 shows the temporal evolution of the average ion charge state $\mathcal{Q}$ obtained for an Ar_6 cluster illuminated by pulses of two different intensities: $I=1.4\times10^{15}$ W/cm^2 (or $\mathcal{F}_0=0.2$ a.u.) and $I=1.3\times10^{16}$ W/cm^2 (or $\mathcal{F}_0=0.6$ a.u.). The inset presents analogous results obtained for an isolated argon atom subjected to the same laser pulses. The charge of the ions is calculated in the following way: for each pseudoparticle its charge is added to the charge of the closest ion; pseudoparticles that are further from any ion than 10 a.u. are considered lost. It is seen that for such a small cluster most ionized electrons leave the cluster during the beginning stages of the pulse. Moreover, it follows from comparison with the inset that the impact of such laser-driven electrons on the explosion process via the mean field is important even in clusters as small as six atoms. Notice that the final charges of the ions from Fig. 8 are similar to the charges obtained recently in Monte Carlo simulations (see, e.g., [12,65]). This proves that the time-dependent Thomas-Fermi model is also able to give also correct quantitative predictions about the process of explosion of rare-gas atomic clusters.

VI. SUMMARY

The dynamics of small rare-gas atomic clusters ionized by a high-intensity femtosecond laser pulse have been studied qualitatively using a three-dimensional refinement of the time-dependent Thomas-Fermi model. It was confirmed that the explosion is neither instantaneous nor uniform. It exhibits a layerlike structure in which shells of cluster ions are expelled sequentially. It seems that the inner shells of the cluster start to expand first and ''push'' the outer shells. The stepwise character of the explosion was seen also in the kinetic energy of the outgoing atomic ion fragments: the ions leaving first were far more energetic than those leaving later. The role of hot electron dynamics in the cluster explosion at the initial stages has also been investigated. It turned out that ions coming from the outer shells of the cluster are indeed somewhat accelerated by thermal expansion of the electron gas. On the other hand, the thermal expansion of the electron gas causes the electrons to leave the inside of the cluster rapidly. This slows down the rate of space-charge ionization inside the cluster and thus the Coulomb explosion of the inner shells is decelerated. Contrary to previous belief, it seems that the hydrodynamic explosion scenario is important for most energetic ions only. The expansion of slower ions from inner shells is governed mainly by the Coulomb forces. The model used was also checked to give correct quantitative predictions in the case of small argon clusters.

ACKNOWLEDGMENTS

M.R. is grateful to Didier Normand for his kind invitation to CEA/Saclay. We thank Maciej Lewenstein for many stimulating discussions and encouragement during the initial phase of this work. We also acknowledge Jaś Mostowski for providing us with his computer resources.

[1] M. Protopapas, C.H. Keitel, and P.L. Knight, Rep. Prog. Phys. **60**, 389 (1997).
[2] T. Ditmire *et al.*, Phys. Rev. A **53**, 3379 (1996).
[3] A. McPherson *et al.*, Nature (London) **370**, 631 (1994).
[4] A. McPherson *et al.*, Phys. Rev. Lett. **72**, 1810 (1994).
[5] T. Ditmire, T. Donnelly, R. Falcone, and M. Perry, Phys. Rev. Lett. **75**, 3122 (1995).
[6] E.M. Snyder, S.A. Buzza, and A.W. Castleman, Jr, Phys. Rev. Lett. **77**, 3347 (1996).
[7] M. Lezius, S. Dobosz, D. Normand, and M. Schmidt, J. Phys. B **30**, L251 (1997).
[8] T. Ditmire *et al.*, Nature (London) **386**, 54 (1997).
[9] M. Lezius, S. Dobosz, D. Normand, and M. Schmidt, Phys. Rev. Lett. **80**, 261 (1998).
[10] Y.L. Shao *et al.*, Phys. Rev. Lett. **77**, 3343 (1996).
[11] T. Ditmire *et al.*, Phys. Rev. Lett. **78**, 2732 (1997).
[12] T. Ditmire, Phys. Rev. A **57**, R4094 (1998).
[13] B.D. Thompson, A. McPherson, K. Boyer, and C.K. Rhodes, J. Phys. B **27**, 4391 (1994).
[14] S. Dobosz *et al.*, Phys. Rev. A **56**, R2526 (1997).
[15] C. Rose-Petruck, K.J. Schafer, K.R. Wilson, and C.P.J. Barty, Phys. Rev. A **55**, 1182 (1997).
[16] K. Boyer, B.D. Thompson, A. McPherson, and C.K. Rhodes, J. Phys. B **27**, 4373 (1994).
[17] F. Calvayrac, P.-G. Reinhard, and E. Suraud, J. Phys. B **31**, 5023 (1998).
[18] S. Kümmel, M. Brack, and P.-G. Reinhard, Phys. Rev. B **58**, R1774 (1998).
[19] P. Blaise, S.A. Blundell, and C. Guet, Phys. Rev. B **55**, 15 856 (1997).
[20] L. Plagne *et al.*, Phys. Rev. A **61**, 033201 (2000).
[21] M. Brewczyk, C.W. Clark, M. Lewenstein, and K. Rzążewski, Phys. Rev. Lett. **80**, 1857 (1998).
[22] M. Brewczyk and K. Rzążewski, Phys. Rev. A **60**, 2285 (1999).
[23] K.C. Kulander, Phys. Rev. A **36**, 2726 (1987).
[24] J. Parker *et al.*, J. Phys. B **29**, L33 (1996).
[25] A. L'Huillier, K.J. Schafer, and K.C. Kulander, J. Phys. B **24**, 3315 (1991).
[26] J.L. Krause, K.J. Schafer, and K.C. Kulander, Phys. Rev. Lett. **68**, 3535 (1992).
[27] J.L. Krause, K.J. Schafer, and K.C. Kulander, Phys. Rev. A **45**, 4998 (1992).
[28] P. Hohenberg and W. Kohn, Phys. Rev. **136**, B864 (1964).
[29] W. Kohn and L.J. Sham, Phys. Rev. **140**, A1133 (1965).
[30] L.H. Thomas, Proc. Cambridge Philos. Soc. **23**, 542 (1926).
[31] E. Fermi, Z. Phys. **48**, 73 (1928).
[32] N.H. March, in *Theory of the Inhomogeneous Electron Gas*, edited by S. Lundqvist and N. March (Plenum, New York, 1983), pp. 1–77.
[33] L. Spruch, Rev. Mod. Phys. **63**, 151 (1991).

[34] K. Huang, *Statistical Mechanics* (Wiley, New York, 1963).
[35] N.D. Mermin, Phys. Rev. **137**, 1441 (1965).
[36] T. Błeński and B. Cichocki, Phys. Rev. A **41**, 6973 (1990).
[37] E. Teller, Rev. Mod. Phys. **34**, 627 (1962).
[38] N.L. Balàzs, Phys. Rev. **156**, 42 (1967).
[39] J. Farges, M.F. de Faraudy, B. Raoult, and G. Torchet, J. Chem. Phys. **78**, 5067 (1983).
[40] J. Farges, M.F. de Faraudy, B. Raoult, and G. Torchet, J. Chem. Phys. **84**, 3491 (1986).
[41] J.A. Northby, J. Chem. Phys. **87**, 6166 (1987).
[42] E.D. Potter, Q. Liu, and A.H. Zewail, Chem. Phys. Lett. **200**, 605 (1992).
[43] E. Runge and E.K.U. Gross, Phys. Rev. Lett. **52**, 997 (1984).
[44] G.D. Mahan and K.R. Subbaswamy, *Local Density Theory of Polarizability* (Plenum, New York, 1990).
[45] E.K.U. Gross and W. Kohn, Adv. Quantum Chem. **21**, 255 (1990).
[46] C.A. Ullrich, U.J. Gossmann, and E.K.U. Gross, Phys. Rev. Lett. **74**, 872 (1995).
[47] E.K.U. Gross, J.F. Dobson, and M. Petersilka, *Density Functional Theory of Time-Dependent Phenomena* (Springer, Berlin, 1996).
[48] K. Burke and E.K.U. Gross, in *Density Functionals: Theory and Applications*, edited by D. Joubert (Springer, Berlin, 1998).
[49] C.A. Ullrich, S. Erhard, and E.K.U. Gross, in *Super Intense Laser Atom Physics IV*, edited by H.G. Muller (Kluwer, Dordrecht, 1996).
[50] X.-M. Tong and S.-I. Chu, Phys. Rev. Lett. **57**, 452 (1998).
[51] F. Bloch, Z. Phys. **81**, 363 (1933).
[52] J.A. Ball, J.A. Wheeler, and E.L. Fireman, Rev. Mod. Phys. **45**, 333 (1973).
[53] K. Ishikawa, B.U. Felderhof, T. Blenski, and B. Cichocki, J. Plasma Phys. **60**, 787 (1991).
[54] L.B. Lucy, Astron. J. **82**, 1013 (1977).
[55] R. Gingold and J. Monaghan, Mon. Not. R. Astron. Soc. **181**, 375 (1977).
[56] W. Benz, in *The Numerical Modeling of Nonlinear Stellar Pulsations*, edited by J.R. Buchler (Kluwer, Dordrecht, 1990), pp. 269–288.
[57] J.J. Monaghan, Annu. Rev. Astron. Astrophys. **30**, 543 (1992).
[58] A.W. Appel, SIAM (Soc. Ind. Appl. Math.) J. Sci. Stat. Comput. **6**, 85 (1985).
[59] J.E. Barnes and P. Hut, Nature (London) **324**, 446 (1986).
[60] L. Greengard, Comput. Phys. **4**, 142 (1990).
[61] L. Greengard, Science **265**, 909 (1994).
[62] L. Hernquist and N. Katz, Astrophys. J., Suppl. Ser. **70**, 419 (1989).
[63] J.K. Salmon, M.S. Warren, and G.S. Winckelmans, Int. J. Supercomput. Appl. **8**, 129 (1994).
[64] W.H. Press, S.A. Teukolsky, W.T. Vetterling, and B.P. Flannery, *Numerical Recipes in FORTRAN* (Cambridge University Press, Cambridge, 1992).
[65] K. Ishikawa and T. Blenski, Phys. Rev. A **62**, 063204 (2000).